Performance Evaluation of LTE-CommSense System for Discriminating the Presence of Multiple Objects in Outdoor Environment

Santu Sardar*, Amit K. Mishra†, *Senior Member, IEEE* and Mohammed Zafar Ali Khan‡, *Senior Member, IEEE* *ANURAG, Defence Research & Development Organization, India †Department of Electrical Engineering, University of Cape Town, South Africa ‡Department of Electrical Engineering, IIT Hyderabad, India

I. INTRODUCTION

Recently there has come an upsurge in activities in the field of using communication radiation for target detection and tracking using receiver only nodes ([1], [2], [3], [4], [5]). Using the same principle, our group has been working for the past few years on a novel remote sensing instrument which works by analyzing the channel equalization process of telecommunication systems. We call it communication based sensing or CommSense ([6], [7], [8]). We have shown that CommSense system can be used to distinguish different weather events, presence and absence of objects and changes in the immediate environment. In case of LTE-CommSense, it uses the Long-Term Evolution (LTE) downlink (DL) signal from the base station (BS) to the user equipment (UE) to extract the channel information and estimate environment change ([8], [9]). The reference pilot symbols transmitted at periodic intervals by the LTE base station or $eNodeB$ [10] for channel estimation and subsequent equalization purpose gets channel-affected while passing through the communication channel. From receiver channel estimation block LTE-CommSense instrument [8] first obtains the channel properties in between $eNodeB$ and UE. The channel estimation block finds the channel impulse response (CIR) which represents the properties of the dynamic channel [11]. It can be noted here that the CommSense type of sensing does not need any dedicated transmitter contrary to the proposals in ([12], [13], [14], [15], [16]) and hence does not need to adhere to transmitter related regulations. The major novelty of CommSense lies in the fact that compared to existing systems ([17], [18], [19]) on localization using WiFi or GSM, in our case we are using no transmitter and it is purely based on pilot carriers only.

In some of the previous reports from our work on CommSense we have shown some encouraging results using both GSM and LTE telecommunication standards ([7], [8], [20], [21]). However, we have not done a formal analysis of the performances of this newly proposed instrument. In the current paper, we apply LTE-CommSense for detection of presence of object in outdoor environment. After that, it was investigated that, whether it can detect and distinguish multiple objects or not. To perform that, we have identified the important figures of merit suitable for LTE-CommSense instrumentation scheme. The figures of merit which we believe to be the most important in this scenario are accuracy of detection, false acceptance rate (FAR), false rejection rate (FRR) and resolution. The concept of resolution is redefined as per the CommSense working philosophy [22] of detecting events instead of objects. CommSense is targeted to detect environmental changes. Types of environmental change will depend on the exact type of application the CommSense instrument needs to detect. For the application in hand, the event may be defined as presence or absence of an object in the immediate outdoor environment. We proposed

two methods to evaluate the resolution for LTE-CommSense viz. Neyman Pearson (NP) principle based resolution and Cramer Rao (CR) principle based resolution from two different vantage points.

This paper is organized as follows. In Section 2, the basic concept of LTE-CommSense is summarized. All the identified characterization parameters and need of redefinition and proposed resolution concept is explained in Section 3. This section also provides two potential proposed definitions of resolution of LTE-CommSense. Section 4 elaborates the experimental procedure to collect the data for detection and distinction of presence of multiple objects practically. The results, evaluated figures of merit, analysis of the extracted data and procedure of calculation of resolution according to the proposed definitions are detailed in Section 5. Section 6 provides the conclusion from these efforts.

II. LTE-COMMSENSE SYSTEM

General block diagram and description of LTE-CommSense are elaborated in ([21], [8]). Figure 1 provides a part of the complete conceptual system described in ([21], [8]) using single UE which is implemented and utilized for this work.
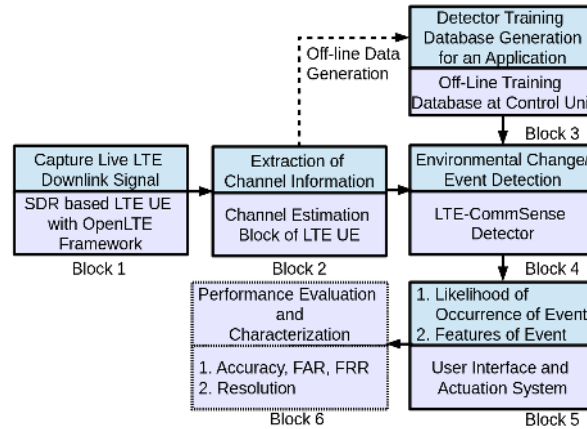

Fig. 1. LTE-CommSense instrumentation system block diagram using single UE.

There are two parts of processing in the system: one is offline and the other one is online. Offline processing chain contains blocks 1, 2, 3 and 4 whereas online processing contains block 1, 2, 4 and 5 in consecutive order. Processing block 6 is particular to this work of characterization. A brief description of individual blocks are as follows.

- Block 1: This block first detects and then captures LTE DL signal from the $eNodeB$ using the USRP N200 software defined radio (SDR) platform, configured as an LTE UE by the use of OpenLTE framework. This block is used both in offline and online modes.
- Block 2: In the LTE UE receiver work-flow, the channel estimation block extracts the channel information from the channel affected cell specific reference symbols (cellRS). The objective of this block is to tap in to the channel estimation block of the UE to capture the extracted channel information. This block is also used both in offline and online mode.
- Block 3: It is used only in offline mode. Based on the target application of object presence detection in outdoor environment and distinguishing presence of multiple objects, we first record LTE DL signal. Using the captured DL data, we have to perform LTE channel estimation and equalization to extract channel impulse response (CIR). Using the CIR values, we have to generate the database to train the LTE-CommSense detector. Data corresponding to multiple capture of application scenarios are used to generate the training database and maintained in the control unit. The control unit tunes LTE-CommSense for targeted application.
- Block 4: This is the LTE-CommSense detector and used in both modes of operation. First, it works in offline mode and gets trained by the application specific database provided by the control unit in

'Block 3'. After that in online mode, it accepts a channel information corresponding to a DL signal capture of current channel condition. The objective of the detector is to give decision of regarding the environmental change or event detection as per the targeted application. Support vector machine (SVM) based classifier is used for the training and testing in this block. It may be replaced with another classifier depending on the application at hand [23].

- Block 5: This block conveys the decision of the detector to the user to take further action by the actuation system. This block works only in online mode. It contains the likelihood of the event occurrence. If the event has occurred, then this block may also provide relevant features of it. In the present case, first this block provides decision regarding presence or absence of an object. If present, it provides further decision of how many objects are present.
- Block 6: This block is for system performance analysis and characterization of LTE-CommSense for the targeted application.

A. Feasibility of Using LTE Reference Signals as Bi-Static Radar Waveform

To detect environmental changes using LTE communication infrastructure, another alternative approach is to utilize the infrastructure as a conventional bi-static radar system. The static base station (BS) i.e. $eNodeB$ will work as the transmitter and UE is the receiver. To utilize it as a radar system, we need a reliable precision clock to find out the time difference between the direct DL signal path from $eNodeB$ to LTE UE and the scattered path from the target. Figure 2 shows the configuration of the base station, user equipment and the relative position of the target. According to the calculations described in Appendix, can be evaluated as shown in Table I. One alternative would be to utilize the clock signal sent by the LTE base stations. System information block (SIB) 16, available for LTE releases 11 onwards, contains Coordinated Universal Time (UTC). As per the standard, the precision of UTC time in this '$SIB - 16$' is $10ms$. We made some simple calculations to check if this is precise enough for us.
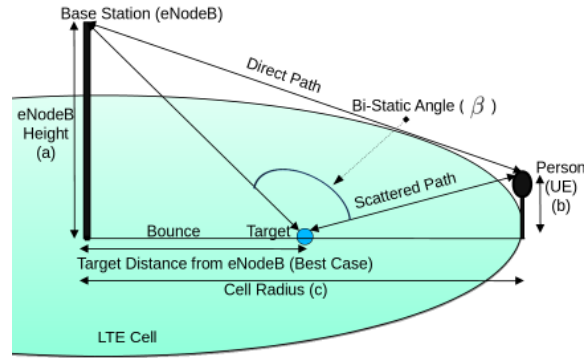

Fig. 2. Best Case Scenario for the calculation of Time Resolution Requirement to use LTE signal in Conventional Radar Framework

It can be observed from Table I that, the timing precision requirements for the best case scenario of detecting a target (Figure I) are higher than the LTE specifications [24]. Therefore, LTE reference signals may not be suitable to use as conventional radar. Hence we investigated alternate ways to extract usable information from the channel data. Without reliable clock we can not use the conventional definition of resolution. As shall be described later, we define alternate definitions of resolution to validate the performance of our system.

III. CHARACTERIZATION PARAMETERS

A. Detection Accuracy, FRR and FAR

For this detector system, the accuracy ([25], [22]) denotes the extent with which the system provides correct detection output i.e. the system's ability to distinguish between presence and absence of the object in outdoor environment.

TABLE I
TIMING PRECISION REQUIREMENTS FOR DIFFERENT TYPES OF LTE CELL AND BASE STATIONS TO USE LTE DOWNLINK REFERENCE
SIGNALS IN CONVENTIONAL RADAR FRAMEWORK.

BS Type	Cell Type	Best Case Timing Precision Requirement
Wide Area	Small	79.9ps (3km radius)
Wide Area	Large	39.9ps (6km radius)
Home Area	Small	0.48ns (0.5km radius)
Home Area	Large	0.24ns (1km radius)

Another two standard measures to indicate the identifying power of a detection methodology are FRR or false negative rate (Type I Error) and FAR or false positive rate (Type II Error) [26]. FAR is fraction of the falsely accepted patterns divided by the number of all impostor patterns. The fraction of the number of rejected client patterns divided by the total number of client patterns is called FRR.

The frequency at which false acceptance errors are made can be denoted as FAR. If N_{FA} is the number of false acceptance cases and N_{IA} is the total number of impostor attempts, then FAR can be defined as:

$$FAR = \left(\frac{N_{FA}}{N_{IA}}\right) \tag{1}$$

Similarly, false rejection is the act of deciding that a category is an impostor while the category is actually genuine. The frequency at which false rejection are made is called FRR. If N_{FR} is the total number of failse rejections, and N_{EA} is the total number of legitimate classification attempts, then FRR can be given as:

$$FRR = \left(\frac{N_{FR}}{N_{EA}}\right) \tag{2}$$

B. Resolution: Conventional Range Resolution and Proposed Redefinition

The definition of resolution for any generic instrument according to the Measurement Systems Analysis Manual is: "the resolution of an instrument is δ if there is an equal probability that the indicated value of any artifact, which differs from a reference standard by less than δ, will be the same as the indicated value of the reference". Therefore generic instruments measure the "value of any artifact" [27]. This general definition of resolution is applicable to any instrument. For a radar system we measure radar range resolution. For a bi-static radar system where the communication base-station antenna is considered to be the transmitter and the user equipment (UE) to be the receiver, we can find out the range resolution. According to general bi-static radar theory, range resolution of this LTE based commensal radar can be defined by:

$$\Delta R = \frac{c}{2 * B * \cos(\frac{\beta}{2})} \tag{3}$$

Here, β is called bi-static angle i.e. the angle the target object makes between the base station transmitter and the UE. The term B denotes the signal bandwidth.

This conventional definition of 'Resolution' is not applicable directly in this case because this instrument is not a conventional radar. Here we are not detecting objects; rather we are distinguishing events. In the analysis presented in this paper, the event is defined as: "Detection of the presence of objects in outdoor environment". Additionally if presence of object is ascertained, then this instrument will estimate the number of objects present. Therefore, there is a basic difference between resolution of conventional object detector as detailed in Equation 3 and CommSense based environment change detector [27]. Instead of processing of radio frequency (RF) data, here the estimated channel impulse response (CIR) is used to

distinguish events occurring in the channel. It should also be event dependent. Therefore 'Resolution' has to be redefined here. As the objective is to distinguish events, the 'Resolution' should be defined with respect to events. Consequently, the value of β is not required here. Therefore direct comparison of the 'Resolution' of LTE-CommSense with the traditional range resolution equation may not be relevant. The resolution of LTE-CommSense may be represented by making use of two different models:

1) Neyman-Pearson Principle based Definition: LTE-CommSense provides a likelihood or probability, P_p which signifies that a certain 'artifact of interest' is present. Let us represent the artifact of interest as θ. For a given task there will always be cases of misclassification which will create events of false alarm giving a probability of false present, P_{fp} . Then using Neyman Pearson [27] criteria, the goal of designing an LTE-CommSense detector is to maximize P_p for a given P_{fp}.

Therefore, using Neyman Pearson principle, resolution (δ_{NP}) can be defined as the maximum change in the artifact of interest, $\Delta\theta$, which for a given LTE-CommSense detector makes sure that the change in the probability of false present $\Delta P_{fp} \leq$ an arbitrary small number.

Definition 1: The Neyman Pearson principle based resolution (δ_{NP}) can be defined as the maximum change in the artifact of interest, $\Delta\theta$, for which the change in the probability of false present $\Delta P_{fp} \leq \epsilon$, ϵ being an arbitrary small number.

2) Cramer-Rao Bound based Definition: From a data-centric point of view for an 'artifact of interest', θ, we may view the LTE-CommSense detector system of LTE-CommSense to capture some signal ζ. One of the major empowering concept of LTE-CommSense detector is the hypothesis that we can estimate θ from ζ even when the exact phenomenological link from θ to ζ is not well-modeled. Therefore, LTE-CommSense detector operation becomes necessarily a parameter-estimation operation. Now, in parameter estimation, one of the important figures of merit is the Cramer Rao lower bound (CRLB) which is the lowest variance [27] achievable in the estimate. According to the statement of the Cramer Rao theorem, if $\hat{\theta}$ is an unbiased estimator of θ, then,

$$Var(\hat{\theta}) \geq \frac{1}{I(\theta)} \tag{4}$$

Here, $I(\theta)$ is a measure of average information and represented by Fisher information. Fisher information statistic can be expressed as:

$$I(\theta) = E\left[\left(\frac{\partial l(\zeta;\ \theta)}{\partial \theta}\right)^2\right] \tag{5}$$

where $l(\zeta;\ \theta)$ is the natural logarithm of the likelihood function and E represents the expectation operation. For ill-defined mapping like what we deal within LTE-CommSense detector, Fisher information can be found numerically. The lower bound shown in Equation 4 is achieved for an unbiased estimator of θ. Therefore to obtain the Cramer Rao principle based resolution of LTE-CommSense, it is required to find the minimum variance of the estimator from measured data.

Definition 2: The Cramer-Rao principle based resolution (δ_{CR}) can be defined as the maximum change in the 'artifact of interest', $\Delta\theta$, for which the change in the inverse of Fisher information $(\Delta I(\theta))$ or the variance of the estimate is less than or equal to an arbitrary small number ϵ.

IV. EXPERIMENTAL SETUP

The objective of this set of practical experiments is to detect the presence or absence of objects in outdoor environment. If detected, this proposed system should further determine whether one or two targets are present. We derive the performance parameters and figures of merit along with the redefined resolution methodically for LTE-CommSense scenario from practical experiment for this case.
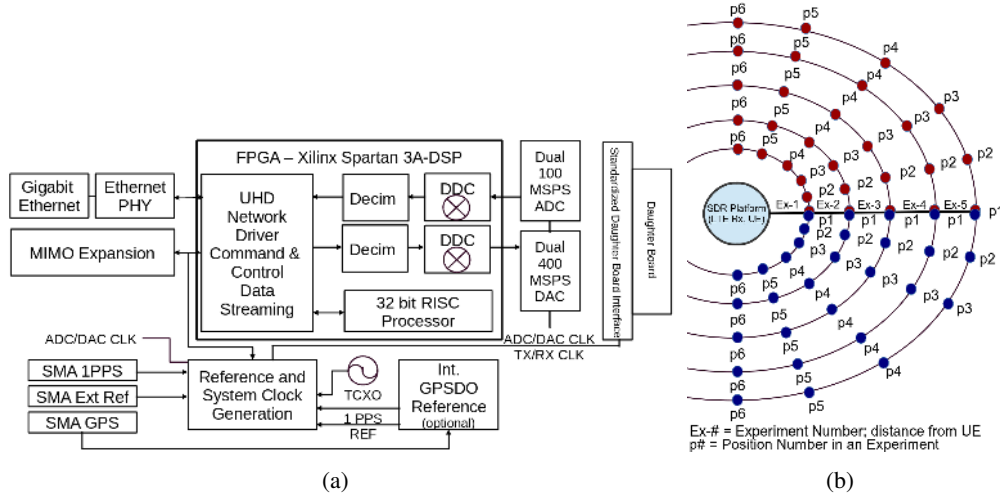
Fig. 3. (a) USRP N200 Internal Block Diagram, (b) Experimental Setup to Calculate Resolution: The SDR based LTE UE is located at the center of the concentric circles. These concentric circles represents different distances of the reflectors from the UE. For each specific distance of the reflectors from the UE, six different readings were taken ($p1, p2, p3, p4, p5, p6$). The small red and blue filled circles are the locations of the reflectors. For these six cases, LTE DL signal is captured by the UE.

To obtain live LTE downlink signal, SDR based data capturing system was developed. USRP N200 SDR platform [28] and RFX2400 RF daughter card [29] along with VERT2450 antenna [30] was used to work at LTE passband operating frequency range. A GNURadio based open source model of the 3GPP LTE receiver on OpenLTE [31] was utilized to control the SDR platform. The internal block diagram of USRP SDR platform is shown in Figure 3(a). The SDR unit was connected to the host computer via Ethernet. The OpenLTE framework was implemented on the host computer. The commands for searching of live LTE DL signal, capturing detected LTE DL data on the host computer for a specified time duration were also input to the SDR platform via host PC using the OpenLTE framework. The LTE UE receiver works at $Band - 40$ (2300 MHz to 2400 MHz frequency band) in time division duplexing (TDD) topology. Figure 3(b) shows the SDR platform, relative placements of the objects for this experiment. Corner reflectors are considered in this practical experiment as reflectors. In this figure, the details of the "*SDR platform (LTE Rx, UE)*" at the middle of the setup is shown in Figure 3(a). The details of the reflectors configuration and their placements are described as follows.

A. Reflectors Configuration and Their Relative Placement

In this work, the objective is to evaluate performance of the LTE-CommSense instrument in detecting presence or absence of objects. If presence is detected, it should also predict the number of objects. In this experiment, we have targeted to detect and distinguish two objects. Therefore we have used two corner reflectors as our targeted objects. These two reflectors are placed at different distances from each other and from the modeled LTE UE to experiment about the distinguishing ability of LTE-CommSense.

Corner reflectors have the advantage of having very high radar-cross-section (RCS) for relatively smaller size and the RCS is maintained over a wide range of incident angle. They are easy to make from metallic sheet such as Aluminum (Al). But care must be taken to ensure that the surfaces are joined at exactly 90° degrees. Also, they should be robust enough to maintain good flatness. In this case, the reflectors are metallic sheets made of Aluminum (Al) with properly perpendicular faces.

The size of the reflectors should be based on the wavelength of the LTE DL signal. The carrier frequency (f) of LTE is 2.1 GHz [32]. Therefore, if the corresponding wavelength is denoted by λ, the relation between f and λ is: $\lambda * f = C$. Here, C is the speed of light in vacuum i.e. $C = 3 * 10^8$ m/s. Therefore,

$$\lambda = \frac{C}{f} = \frac{3 * 10^8}{2.1 * 10^9} = 0.14m \qquad (6)$$

We observe that, the wavelength of the LTE DL signal will be in the range of $0.14m$. The size of each face is made five times more to ensure sufficient amount of reflected signal is reflected and received by the modeled LTE UE terminal on the SDR platform.

As shown in Figure 3(b), two different reflectors were placed at different distances from each other and different distances from UE. The environment selected was outdoor open field environment. Data were collected for one reflector and two reflectors cases. Five different distances of the reflectors from the UE were considered viz. $0.5m$, $2m$, $4m$, $7m$ and $10m$. For each of the distances, intra-reflector distances of the two reflectors were varied along the circumference of the circle with the radius to be the distance from the UE and center at the UE position. Six different intra-reflector distances were considered as per the formula:

$$S = x * \pi * D \tag{7}$$

Here D was the distance of the reflectors from the UE and x was a number which has assumed the values 0.00, 0.10, 0.25, 0.50, 0.75 and 1.00 respectively during the experiment. This distance was along the circumference of the circle which has D as the radius. Correspondingly the straight line distance between the reflectors can be found using:

$$D_{intra} = 2 * D * \sin\left(\frac{S}{2 * D}\right) \tag{8}$$

Here, D_{intra} was the straight line distance between the two reflectors, D was the radius of the circle i.e. distance of the reflectors from the UE and S was the distance of the reflectors along the circumference of the circle.

V. RESULTS AND ANALYSIS

Using the experimental setup, the primary figures of merit viz. accuracy of detection of targeted event, FRR and FAR are evaluated first. Then, these are used to evaluate the resolution of LTE-CommSense instrument as per the proposed definitions.

A. Figures of Merit

Figure 4(a) shows the variation of the average values of accuracy w.r.t. the absolute distance between the reflectors as well as their distances from the UE. The X axis shows the distances (m) of the reflectors from the UE whereas the Y axis shows the absolute distance (m) between the reflectors. In this figure, the accuracy corresponding to every distance point is indicated. It can be observed that, for a particular distance of the reflectors from the UE, as the distance between the reflectors increases, the accuracy of distinguishing between single reflector and double reflector case also increases and it reaches its maximum when the two reflectors are diagonally opposite which is the maximum distance between them for a particular distance of the reflectors from the UE. It can be also observed that, if the reflectors are very close $(0.5m)$ to UE or very far $(10m)$ from UE, the performance accuracy decreases.

Figure 4(b) shows the variation of average accuracy w.r.t. the intra reflector distance for a particular distance of the reflectors from the SDR based LTE UE. The distances of the reflectors from the UE are fixed to be $4m$ here. Six different intra reflector distances are considered as explained earlier. The absolute straight line distances between the reflectors are $0.00m$, $2.50m$, $3.06m$, $5.65m$, $7.39m$ and $8.00m$ respectively. It can be observed from the figure that as the distance between the reflectors increases, the accuracy increases. This means that the capability of LTE-CommSense to distinguish between two reflector case also increases.

In the next case, we keep the reflectors diagonally opposite and vary the distance (D) of them from the SDR based LTE UE. Data is collected for five different distances of the reflectors from the UE viz. $0.5m$, $2m$, $4m$, $7m$ and $10m$. It can be observed from Figure 4(c) that, if the reflectors are very

close to UE ($0.5m$), the accuracy is lower. This is due to the reason that, the absolute distance of the reflectors will be very less. Therefore, it is difficult for CommSense to distinguish between single and double reflectors. Up to $7m$ distance, the accuracy is $\sim 90\%$ but beyond that the accuracy decreases gradually. This is mainly due to the fact that, LTE-CommSense utilizes communication infrastructure and the operating signal to noise ratio (SNR) for a communication system is lower than that of a radar system. For LTE communication system, typical SNR level is $\sim 7dB$ for a fair signal quality whereas, radar operation at long ranges requires SNR of $\sim 25dB$ [33]. If higher accuracy is required beyond $10m$ for LTE-CommSense instrument, then the operating SNR level has to be improved further. This demands modification in the communication infrastructure being used for CommSense which is against its basic principle. Additionally, as the distance between this passive instrument and the object of interest increases further, environmental effects viz. fading, noise, received signal strength, near range ground bouncing, multi-path reflections form nearer objects etc.) will dominate the received signal as can be seen from [34]. This will decrease the accuracy gradually with respect to increase of distance. Increasing the size of the reflector should further increase the range over which the accuracy is more than 90%.

A detection methodology should optimize both FAR and FRR. Figure 4(d) shows the FAR and Figure 4(e) the FRR values with respect to the distances of reflector from the SDR based LTE UE. It can be observed that, FAR are very less and FRR are very high when the distance between them are less because, in that type of situation. it is difficult for the CommSense device to distinguish between single and double reflector case. Gradually FAR increases up to a maximum of 0.16 for $7m$ distance between the reflectors and the UE. But as the distance between the UE and the reflectors increases further, e.g. for $10m$ distance, FAR decreases. This is due to the fact that, as distance increases, less amount of DL signals are reflected back to the UE by the reflectors. We also observe that, as the distance between them increases, FRR gradually decreases.

B. Derivation of Resolution according to Neyman Pearson Criteria

Using Neyman-Pearson principle, resolution (δ_{NP}) is the maximum change in the 'artifact of interest', $\Delta\theta$, to ascertain that the change in the false present rate $\Delta FAR \leq$ an arbitrary small number. We consider the change in the distance between the reflectors as the 'artifact of interest'. From the figure on FAR for this experiment (Figure 4(d)), changes in the intra reflector distances and corresponding FAR changes for a particular distance of the reflectors from the UE can be recorded. Cases of no FAR value changes corresponding to maximum distance change between the reflectors for different distances from the UE can be evaluated from that. We observed that, for our proposed instrument, when the distance from UE is $0.5m$ and the distance of the reflectors are $0.3827 \approx 0.38m$ along the circumference of the circle with UE in center and $0.5m$ as radius, the change in the value of FAR is arbitrary small. Also, when the distance between the reflector increases, FAR also increases. Therefore, it can be concluded that, $0.3827 \approx 0.38m$ is the minimum distance change for which the change in FAR value is smaller than any arbitrary small number when the reflectors are $0.5m$ apart from the UE. Following the same logic, the resolution of LTE-CommSense at distances $2m$, $4m$, $7m$ and $10m$ can be evaluated as $1.5m$, $2.5m$, $3m$ and $3.2m$ respectively.

C. Derivation of Resolution according to Cramer Rao Lower Bound Principle

The derivation of Cramer Rao lower bound principle can be found in ([35], [36]). Following 'Definition 2' in Section III-B2, Cramer-Rao principle based resolution is calculated for each value of reflectors distance from user equipment (UE). To perform that we need the probability density function which is estimated as follows. Therefore, total six readings were taken for a particular distance (D) of UE from the reflectors. Similarly five different D values were considered. Additionally one reading were taken for the case of no reflectors were present. Hence, a total of thirty one readings were taken. One LTE frame is of ten milliseconds (ms) duration consisting ten subframes of one millisecond each containing I-Q data. If one recording of LTE DL data is captured for fifteen seconds, we can evaluate up to 1500 different

channel estimates forming 1500 readings from a single recording as per the above procedure. In practice, downlink data were captured more than 15 seconds because a part of the initial data is consumed for timing and frequency offset correction operation. The procedure of timing and frequency offset correction is detailed in the LTE standards ([37], [38], [39]). Therefore, we have 1500 readings for each of the intra reflector distances for each of the thirty one set of captured downlink data.

The accuracy values for each of the above cases are evaluated. For all the cases of distances of the reflectors from the UE and intra reflector distances, the accuracy values assumes a Gaussian distribution with different mean and variance values. From the practical data, the mean, variance and standard deviation of the data are calculated for each case.

For a particular distance of the reflectors from the UE, the steps performed to evaluate the corresponding resolution are summarized in the pseudo-code shown in Algorithm 1. Here the number of different reflector distances from the UE is denoted by M. Also, for every particular reflector distance from UE, the number of considered intra-reflector distances are denoted by N.

The logarithm values ($L(\theta)$) obtained from practical data for different intra reflector distances for a particular distance of the reflectors from the UE, the derivative of $L(\theta)$ obtained for different intra reflector distances for a particular distance of the reflectors from the UE, $\left[\frac{\partial l(\zeta; \theta)}{\partial \theta}\right]^2$ values, expected value of $\left[\frac{\partial l(\zeta; \theta)}{\partial \theta}\right]^2$, Fisher information and variances are calculated using these data.

The CRLB principle based derivation of resolution along with the NP principle [36] based resolution values for different distance of the reflectors from the UE is shown in Figure 4(f). As a comparison, we calculated the conventional range resolution of a bi-static radar system considering LTE $eNodeB$ as the transmitter the LTE UE as the receiver. The available bandwidths in LTE ([38], [39]) are: 5, 10, 15 and 20 MHz [10]. In Figure 4(g), we plotted the conventional bi-static radar range resolution (m) as a function of the bi-static angle for different bandwidths available for LTE communication system. The bi-static angle varies due to the different reflector positions as shown in Figure 3(b).

The following observations can be inferred from the results:

1) The derivation of resolution of LTE-CommSense for NP principle based method and CRLB principle based method yields similar results in this application scenario as is shown in Table II.

2) It can be observed from Figure 4(g) that the conventional radar range resolution depends on the radar operating bandwidths and the bi-static angle corresponding to bi-static configuration. For the bi-static radar scenario, the range resolution is constant when the bi-static angle and the bandwidth is constant. The best resolution is attained for the 20MHz bandwidth. Contrary to that, the CommSense principle based approach cannot provide range or angle information. The proposed resolution of LTE-CommSense is not a constant value. It varies with the distance of the reflectors from the UE.

VI. Conclusion

LTE-CommSense is our proposed environment sensing system. It is a spectrum efficient system because it utilizes the communication spectrum without detrimental effect on it. As no transmitter and related regulations are involved, it can work undetected and may have smaller size and low cost compared to other environment sensing systems which require active transmitters.

This work is an effort to apply the LTE-CommSense system for distinguishing objects in outdoor environment and evaluate the resolution of this system. As the objective of LTE-CommSense is to detect environment change due presence of objects or reflectors, we redefine resolution making 'environment change' as the 'artifact of interest'. We proposed two potential formulations of resolution for LTE-CommSense using Neyman Pearson principle and Cramer Rao lower bound (CRLB) principle.

We have derived the performance parameters using practical data using the detailed experimental setup. LTE DL signal was captured using SDR based LTE receiver implementation with OpenLTE GNURadio framework and two corner reflectors. Multiple LTE DL signal was captured corresponding to different reflector distances from the UE and different intra-reflector distances. LTE-CommSense detector analyzed

---

Algorithm 1: Evaluation of proposed Cramer Rao Lower Bound (CRLB) based 'Resolution' of LTE-CommSense from practical data for multiple object detection in outdoor environment

---

1 <u>function: CRLB-based-Resolution</u> (θ, P, $Resolution$);

   Input : θ: represents intra-reflector distances for different reflector distances from UE, Evaluated pdf (P) for multiple Reflectors Configurations

   Output: $Resolution$: Resolution of LTE-CommSense at different distances from the LTE UE

2 **for** *($i = 0, i < M$; $i++$)* **do**

3   **for** *($j = 0, j < N$; $j++$)* **do**

4   **DO** Derivation of pdf (Curve Fitting)

5   **if** *pdf is Gaussian* **then**

6 $P(\theta_{ij}) = \frac{1}{\sqrt{2\pi}\sigma}e^{-\frac{(\theta_{ij}-\mu_{ij})^2}{2\sigma_{ij}^2}}$

7   **else**

8   Derive parameters for fitted pdf

9   **end**

10   **if** *($P(\theta_{ij}) = \frac{1}{\sqrt{2\pi}\sigma}e^{-\frac{(\theta_{ij}-\mu_{ij})^2}{2\sigma_{ij}^2}}$)* **then**

11 $L(\theta_{ij}) = log_e(P(\theta_{ij})) = log_e(\frac{1}{\sqrt{2\pi}\sigma_{ij}}) - \frac{(\theta_{ij}-\mu_{ij})^2}{2\sigma_{ij}^2}$; % log-likelihoods

12 $\frac{\partial L(\theta_{ij})}{\partial\theta_{ij}} = \frac{\mu_{ij}-\theta_{ij}}{2\sigma_{ij}^2}$; % partial derivatives

13   **E**valuate: $\left[\frac{\partial L(\zeta;\theta_{ij})}{\partial\theta_{ij}}\right]^2$;% square of derivatives

14 $I(\theta_{ij}) = E\left[\left(\frac{\partial L(\zeta;\theta_{ij})}{\partial\theta_{ij}}\right)^2\right]$; % information measure

15 $Var_{ij} = \frac{1}{I(\theta_{ij})}$; % variances of the estimate

16   **else**

17   If pdf not Gaussian, derive above steps for that pdf.

18   **end**

19   **end**

20   **for** *($j = 0, j < N$; $j++$)* **do**

21   **E**valuate: $\Delta\theta_{ij} = \theta_{ij}(M) - \theta_{ij}(M-1)$;% Artifact of Interest

22   **E**valuate: $\Delta Var_{ij} = VAR(\Delta\theta_{ij})$;

23   **if** *($\Delta Var_{ij} < Var_{min}(i)$)* **then**

24 $Var_{min}(i) = \Delta Var_{ij}$;

25   **else**

26 $Var_{min}(i) = Var_{min}(i)$;

27   **end**

28   **for** $Var_{min}(i)$ **do**

29   Find corresponding $\Delta\theta_i$;

30 $Resolution(i) = \Delta\theta_i$; % Resolution at a Particular distance from UE

31   **end**

32   **end**
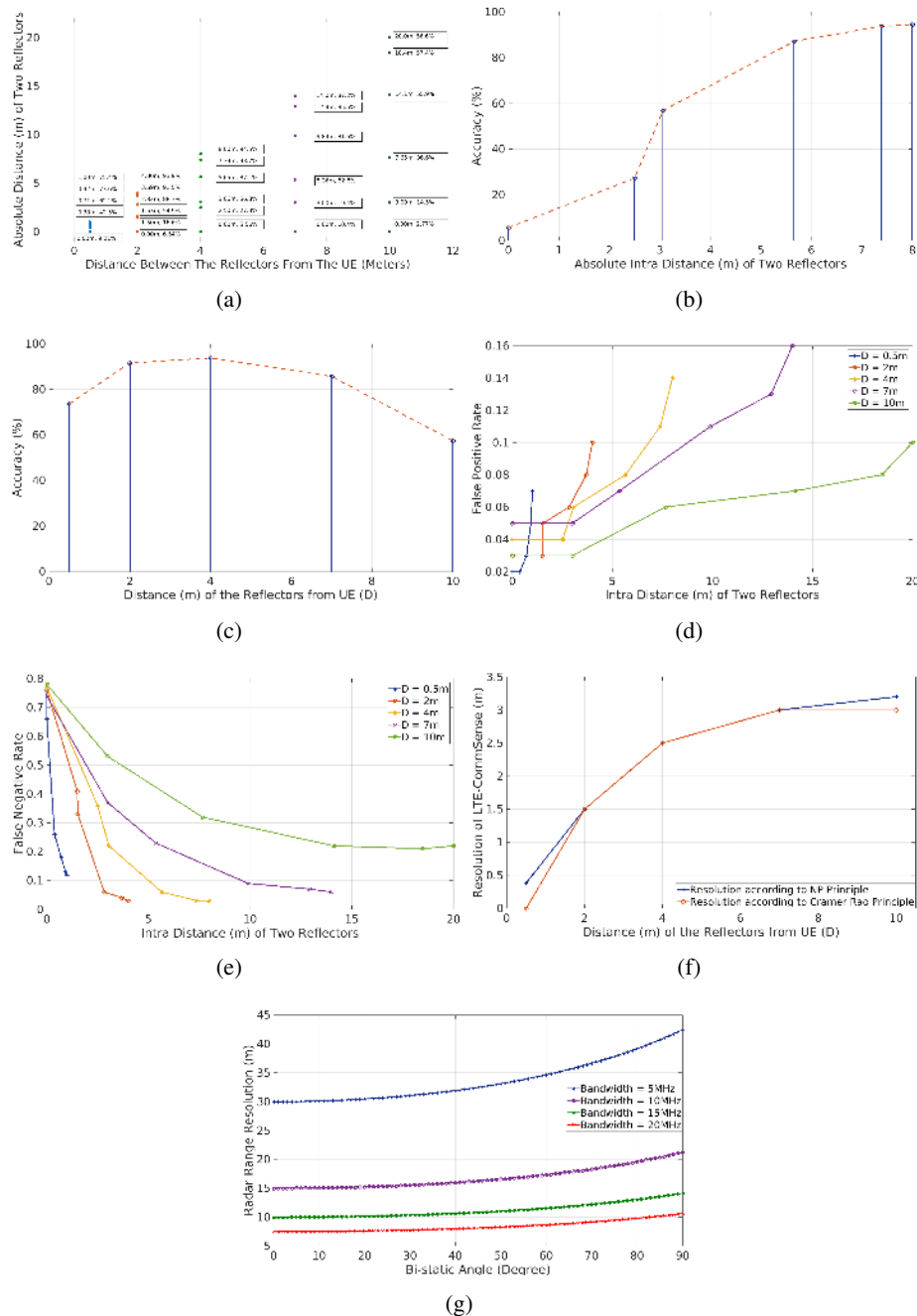
33 **end**

34 return $Resolution$;

Fig. 4. (a) Average Accuracies for Intra Reflector Distances in terms of Absolute Distance (m) from Each Other (in Y axis) for different distances (m) of the reflectors from the UE (in X axis), (b) Variation of Average Accuracy w.r.t. Distance of the Reflectors from Each Other. For this figure, the Distance of both the Reflectors from the UE is kept $04m$. Therefore, using Equation 7 for our experimental setup, the considered distances (S) between the reflectors along the circumference are 0, $1.2564m$, $3.141m$, $6.282m$, $9.423m$ and $15.564m$. Using these values of S in Equation 8, the straight line distances between the reflectors are $0m$, $2.5m$, $3.06m$, $5.65m$, $7.39m$ and $8m$ respectively, (c) Variation of Average Accuracy w.r.t. Distance of the Reflectors from the UE. The Distance between the Reflectors is kept to be $2*D$, where D is the distance of the reflectors from the UE, (d) FAR vs. Intra Reflector Distances in terms of Fraction of the Circumference for different distances of the reflectors from the UE as Diameter, (e) FRR vs. Intra Reflector Distances in terms of Fraction of the Circumference for different distances of the reflectors from the UE as Diameter, (f) Resolution of LTE-CommSense according to Neyman Pearson Principle and Cramer Rao Principle vs. the Distance of the Reflectors from the UE, (g) Bi-Static Radar Range Resolution (m) w.r.t. Bi-static Angle for different LTE Bandwidths. The bi-static angle is the angle exerted by the location of the target between the $eNodeB$ transmitter and UE.

TABLE II
DERIVED RESOLUTION OF LTE-COMMSENSE INSTRUMENT ACCORDING TO THE TWO PROPOSED DEFINITIONS VIZ. NEYMAN PEARSON
BASED AND CRAMER RAO PRINCIPLE BASED DEFINITIONS.

Distance (m) from UE	Resolution according to NP Principle (m)	Resolution according to CR Principle (m)
0.5	0.3827	0.0
2.0	1.5	1.5
4.0	2.5	2.5
7.0	3.0	3.0
10.0	3.2	3.0

these practical data and detector output is utilized to find out accuracy of this environment change detector, FAR and FRR of this system for all the experimental cases. These information were utilized further to evaluate the two proposed LTE-CommSense resolutions for the targeted application according to Neyman Pearson principle and CRLB principle.

While calculating the resolution using Neyman Pearson principle, it was observed that, $0.38m$, $1.5m$, $2.5m$, $3.0m$ and $3.2m$ are the value of the 'artifact of interest' for which the FAR value is the smallest corresponding to UE distances of $0.5m$, $2m$, $4m$, $7m$ and $10m$ respectively. Therefore, the resolution of LTE-CommSense according to the NP principle is $0.38m$, $1.5m$, $2.5m$, $3.0m$ and $3.2m$ corresponding to reflector distances of $0.5m$, $2m$, $4m$, $7m$ and $10m$ from the UE respectively. To calculate the resolution using Cramer Rao principle, we evaluated the variances of the estimates and the same was used to evaluate the resolution according to the proposed definition. It was found that, both the definitions yield similar values of resolution as expected as both the definitions signifies the same characterization parameter. We have compared the evaluated proposed resolution with the conventional radar range resolution for bi-static scenario. For a given bi-static angle and bandwidth, the conventional radar range resolution is constant. But the event dependent proposed resolution of LTE-CommSense detector depends on the distance of the reflectors from the user equipment.

Finally, we can successfully conclude that, LTE-CommSense can be used for object detection in outdoor environment. If detected, it can also distinguish between presence of one object and two objects. The exhaustive performance evaluation for this application using practical data may also serve as a benchmark and may be taken into consideration to apply LTE-CommSense for any other similar application.

REFERENCES

[1] H. Griffiths and C. Baker, "Passive coherent location radar systems. part 1: performance prediction," *Radar, Sonar and Navigation, IEE Proceedings*, vol. 152, no. 3, pp. 153–159, 2005.

[2] M. Inggs and C. Tong, "Commensal radar using separated reference and surveillance channel configuration," *Electronics letters*, vol. 48, no. 18, pp. 1158–1160, 2012.

[3] T. Huang and T. Zhao, "Low pmepr OFDM radar waveform design using the iterative least squares algorithm," *IEEE Signal Processing Letters*, vol. 22, pp. 1975–1979, 2015.

[4] S. D. Domenico, M. D. Sanctis, E. Cianca, P. Colucci, and G. Bianchi, "LTE-based passive device-free crowd density estimation," in *2017 IEEE International Conference on Communications (ICC)*, May 2017, pp. 1–6.

[5] G. Papadopoulos, K. Efstathiou, Y. Li, and A. Delis, "Implementation of an intelligent instrument for passive recognition and two-dimensional location estimation of acoustic targets," *IEEE Transactions on Instrumentation and Measurement*, vol. 41, no. 6, pp. 885–890, Dec 1992.

[6] A. Mishra, "Monitoring changes in an environment by means of communication devices." Google Patents, Oct. 27 2016, WO Patent App. PCT/IB2016/052,235.

[7] A. Bhatta and A. K. Mishra, "GSM-based CommSense system to measure and estimate environmental changes," *IEEE Aerospace and Electronic Systems Magazine*, vol. 32, no. 2, pp. 54–67, February 2017.

[8] S. Sardar, A. K. Mishra, and M. Z. A. Khan, "LTE CommSense for object detection in indoor environment," in *IEEE Aerospace and Electronic Systems Magazine*, Accepted in July 2017.

[9] G. Mois, S. Folea, and T. Sanislav, "Analysis of three iot-based wireless sensors for environmental monitoring," *IEEE Transactions on Instrumentation and Measurement*, vol. 66, no. 8, pp. 2056–2064, Aug 2017.

[10] S. Sesia, I. Toufik, and M. Baker, *LTE - The UMTS Long Term Evolution, From Theory to Practice*. Wiley, 2009.

[11] J. R. Huynen, "A revisitation of the phenomenological approach with applications to radar target decomposition," *DTIC Document, Tech. Rep.*, 1982.

[12] S. Mhlbacher-Karrer, A. H. Mosa, L. Faller, M. Ali, R. Hamid, H. Zangl, and K. Kyamakya, "A driver state detection system combining a capacitive hand detection sensor with physiological sensors," *IEEE Transactions on Instrumentation and Measurement*, vol. 66, no. 4, pp. 624–636, April 2017.

[13] Z. Khan, J. J. Lehtomki, E. Hossain, M. Latva-Aho, and A. Marshall, "An fpga-based implementation of a multifunction environment sensing device for shared access with rotating radars," *IEEE Transactions on Instrumentation and Measurement*, vol. 67, no. 11, pp. 2561–2578, Nov 2018.

[14] H. Zheng, R. Ma, M. Liu, and Z. Zhu, "A linear dynamic range receiver with timing discrimination for pulsed tof imaging ladar application," *IEEE Transactions on Instrumentation and Measurement*, vol. 67, no. 11, pp. 2684–2691, Nov 2018.

[15] H. Lee and K. Ke, "Monitoring of large-area iot sensors using a lora wireless mesh network system: Design and evaluation," *IEEE Transactions on Instrumentation and Measurement*, vol. 67, no. 9, pp. 2177–2187, Sept 2018.

[16] J. Gutirrez, J. F. Villa-Medina, A. Nieto-Garibay, and M. . Porta-Gndara, "Automated irrigation system using a wireless sensor network and gprs module," *IEEE Transactions on Instrumentation and Measurement*, vol. 63, no. 1, pp. 166–176, Jan 2014.

[17] W. Xue, W. Qiu, X. Hua, and K. Yu, "Improved wi-fi rssi measurement for indoor localization," *IEEE Sensors Journal*, vol. 17, no. 7, pp. 2224–2230, April 2017.

[18] C. Chen, Y. Han, Y. Chen, F. Zhang, and K. J. R. Liu, "Time-reversal indoor positioning with centimeter accuracy using multi-antenna wifi," in *2016 IEEE Global Conference on Signal and Information Processing (GlobalSIP)*, Dec 2016, pp. 1022–1026.

[19] C. Chen, Y. Chen, H. Lai, Y. Han, and K. J. R. Liu, "High accuracy indoor localization: A wifi-based approach," in *2016 IEEE International Conference on Acoustics, Speech and Signal Processing (ICASSP)*, March 2016, pp. 6245–6249.

[20] A. Bhatta and A. K. Mishra, "Implementation of GSM channel estimation using open-source SDR environment," in *2015 International Conference on Microwave, Optical and Communication Engineering (ICMOCE)*, Dec 2015, pp. 322–325.

[21] S. Sardar, A. K. Mishra, and M. Z. A. Khan, "LTE-CommSense system and its feasibility analysis," 13th *edition of IEEE AFRICON 2017*, 2017.

[22] G. C. Gill and P. L. Hexter, "Some instrumentation definitions for use by meteorologists and engineers," *IEEE Transactions on Geoscience Electronics*, vol. 11, no. 2, pp. 83–89, April 1973.

[23] Z. Chen and W. Li, "Multisensor feature fusion for bearing fault diagnosis using sparse autoencoder and deep belief network," *IEEE Transactions on Instrumentation and Measurement*, vol. 66, no. 7, pp. 1693–1702, July 2017.

[24] European Telecommunications Standards Institute (ETSI), "LTE; evolved universal terrestrial radio access (E-UTRA); radio resource control (RRC); protocol specification," *ETSI TS 136 331*, vol. 13.0.0, pp. 1–670, 2016.

[25] J. D. Echard, "Estimation of radar detection and false alarm probability," *IEEE Transactions on Aerospace and Electronic Systems*, vol. 27, no. 2, pp. 255–260, Mar 1991.

[26] S. Sardar, G. Tewari, and K. A. Babu, "A hardware/software co-design model for face recognition using Cognimem neural network chip," in *2011 International Conference on Image Information Processing*, Nov 2011, pp. 1–6.

[27] A. K. Mishra, "Application Specific INstrumentation (ASIN): A bio-inspired paradigm to instrumentation using recognition before detection," *CoRR*, vol. abs/1611.00228, 2016.

[28] S. Yun and L. Qiu, "Supporting wifi and LTE co-existence," in *2015 IEEE Conference on Computer Communications (INFOCOM)*, April 2015, pp. 810–818.

[29] *USRP N200/N210 NETWORKED SERIES. http : //www.ettus.com/product/category/Daughterboards/RFX2400*.

[30] *USRP N200/N210 NETWORKED SERIES. http : //www.ettus.com/product/details/V ERT2450*.

[31] N. Nikaein, R. Knopp, F. Kaltenberger, L. Gauthier, C. Bonnet, D. Nussbaum, and R. Ghaddab, "Demo: OpenAirInterface: an open LTE network in a PC," in *MOBICOM 2014, 20th Annual International Conference on Mobile Computing and Networking, September 7-11, 2014, Maui, Hawai*, Maui, UNITED STATES, 09 2014. [Online]. Available: http://www.eurecom.fr/publication/4371

[32] ETSI, "LTE; evolved universal terrestrial radio access (E-UTRA); tdd home enode b (HeNB) radio frequency (RF) requirements analysis," *ETSI TR 136 922*, vol. 9.0.0, pp. 1–78, 2010.

[33] S. H. M. A. Sadoon and B. H. Elias, "Radar theoretical study: Minimum detection range and maximum signal to noise ratio (snr) equation by using matlab simulation program," *American Journal of Modern Physics*, vol. 2, pp. 234–241, July 2013.

[34] P. Krysik, P. Samczynski, M. Malanowski, L. Maslikowski, and K. Kulpa, "Velocity measurement and traffic monitoring using a gsm passive radar demonstrator," *Aerospace and Electronic Systems Magazine, IEEE*, vol. 27, pp. 43–51, 10 2012.

[35] H. L. V. Trees, *Detection, Estimation, and Modulation Theory: Radar-Sonar Signal Processing and Gaussian Signals in Noise*. Melbourne, FL, USA: Krieger Publishing Co., Inc., 1992.

[36] S. M. Kay, *Fundamentals of Statistical Signal Processing: Estimation Theory*. Upper Saddle River, NJ, USA: Prentice-Hall, Inc., 1993.

[37] *http : //www.3gpp.org/ftp/Specs/html − info/36 − series.htm*.

[38] D. et. al., "3g evolution: HSPA and LTE for mobile broadband," *Academic Press*, 2007.

[39] H. E. et al., "Technical solutions for the 3G long-term evolution," *IEEE Commun. Mag.*, vol. 44, no. 3, pp. 38–45, 2006.

VII. Appendix

Figure 2 represents a relative position of the LTE base station, UE and a target inside the cell coverage area. As the objective is to calculate the best case timing precision calculation, the UE is placed at the cell boundary. Let the height of the tower ($eNodeB$) be 'a'; height of the person be 'b'; distance between tower and person be 'c' and the point where the ray bounces off from the target be '*bounce*'. Therefore, distance between the $eNodeB$ top and the target:

$$d1 = \sqrt{a^2 + bounce^2} \tag{9}$$

Distance between the UE and the target:

$$d2 = \sqrt{b^2 + (c - bounce)^2} \tag{10}$$

Distance between the $eNodeB$ top and the UE:

$$d3 = \sqrt{(a - b)^2 + c^2} \tag{11}$$

Therefore, distance difference between direct path and reflected path:

$$\delta = d1 + d2 - d3 \tag{12}$$

We assume the speed of light is $3*10^8$ m/s. Therefore time difference between direct path and reflected path:

$$\Delta t = \delta/(3*10^8) \tag{13}$$

In this work, we have assumed the height of the base station tower ('a') is $10m$ and height of the UE from the ground ('b') to be $2m$. The value of '$bounce$' is considered as half of the distance of the UE from the LTE base station $eNodeB$.